

# Chiral predictions for $K_L \rightarrow \pi^0 \gamma \mu^+ \mu^-$

John F. Donoghue

Department of Physics and Astronomy  
University of Massachusetts, Amherst, MA 01003, USA

and

Fabrizio Gabbiani

Department of Physics  
Duke University, Durham, NC 27708, USA

## Abstract

We have previously analysed the chiral predictions for the decay  $K_L \rightarrow \pi^0 \gamma e^+ e^-$  and discussed how experimental measurements of this process can help our understanding of chiral theories and of CP tests. Motivated by the possibility that the analogous muonic process may soon be measurable, we extend this calculation to the decay  $K_L \rightarrow \pi^0 \gamma \mu^+ \mu^-$ . Branching ratios and differential branching ratios are calculated and presented. Measurements of these will help shed some light on the puzzles in our understanding of the chiral loop effects which were raised by the rate for  $K_L \rightarrow \pi^0 \gamma \gamma$ .

# I. Introduction

The radiative rare kaon decays

$$\begin{aligned}
K_L &\rightarrow \pi^0 \gamma\gamma, \\
K_L &\rightarrow \pi^0 \gamma e^+ e^-, \\
K_L &\rightarrow \pi^0 e^+ e^-, \\
K_L &\rightarrow \pi^0 \gamma \mu^+ \mu^-, \\
K_L &\rightarrow \pi^0 \mu^+ \mu^- 
\end{aligned} \tag{1}$$

form a complex of interrelated processes which share some common features. They can be analysed using chiral perturbation theory [1], and the experimental exploration of the entire complex provides stringent checks on the theoretical methods. Predictions for all of them exist in the literature [2, 3, 4, 5], except for the one that is the subject of this note,  $K_L \rightarrow \pi^0 \gamma \mu^+ \mu^-$ . Our goal is to provide information on this rate and the corresponding decay distributions.

The motivation for studying this decay can best be seen by first considering the reaction  $K_L \rightarrow \pi^0 \gamma\gamma$ . This process takes place dominantly through loop process with pions in the loop. The decay distribution is quite distinctive and the rate is predicted without any free parameters at one-loop order. Interestingly, the distribution agrees well with experiment, but the theoretical rate appears too small by more than a factor of two. In attempting to resolve this, several authors have gone beyond the straightforward one-loop (order  $E^4$ ) chiral calculation. One in particular [3] has added a series of higher order effects in a quasi-dispersive framework and had some surprising success at increasing the rate without modifying the decay distribution greatly. The physics which determines  $K_L \rightarrow \pi^0 \gamma\gamma$  also drives the reaction which we consider in this paper. By studying the leptons plus photon modes experimentally, we are able to achieve independent confirmation of the dynamics that drives this complex of decay modes.

We also are motivated to report our results for this mode by the expectation that it may well be measured in the near future using KTeV at Fermilab [6]. Muons have some experimental advantages compared to electrons, so that although the present decay channel has a smaller branching ratio, the mode may be more readily extracted from the data.

There are two separate calculations that we report on. In the first, we take only the one-loop result within chiral perturbation theory. This gives not only a parameter-free prediction for the rate but also predicts the  $q^2/m_\pi^2$  variation of the amplitude with the invariant mass of the two muons,  $q^2$ . In the second calculation, we add all the ingredients considered in Ref. [3], namely higher order behavior in the experimental  $K_L \rightarrow 3\pi$  decay rate and the effects of vector meson exchanges between the photon vertices. The latter adds a free parameter to the problem, so that it is not surprising that we can modify the rate. However, that parameter is determined by the  $K_L \rightarrow \pi^0 \gamma\gamma$  rate, so for our process it is considered already known. If this mechanism is correct, that same parameter that fixes the rate in one calculation must agree with the rates and energy distributions in all of the related processes.

The resulting formulas are those already presented in [4], but in the phase space integration we substitute the mass of the electron with that of the muon.

In the pure chiral calculation to order  $E^4$  the diagrams are shown in Fig. 1. The result we obtain for the branching ratio up is

$$B(K_L \rightarrow \pi^0 \gamma e^+ e^-) = 4.5 \times 10^{-11}. \tag{2}$$

As in Ref. [4], we define

$$s = (k_1 + k_2)^2, \quad z = \frac{s}{m_K^2}, \quad y = \frac{p_K \cdot (k_1 - k_2)}{m_K^2}. \tag{3}$$

Here  $k_1$  and  $k_2$  are the momenta of the off-shell and on-shell photons, respectively, with the off-shell photon materializing into the muon pair.

The decay distributions in  $z$  and  $y$  provide more detailed information. We present them in Figs. 2 and 3.

At  $\mathcal{O}(E^6)$  the higher order effects in the  $K_L \rightarrow 3\pi$  vertex are extracted from a quadratic fit to the amplitude. These then do not add any new uncertainties to the radiative amplitude. However, vector meson exchange introduces new parameters which measure the strength of the exchange diagram of Fig. 4. In Ref. [3] the result is parametrized by a “subtraction constant” which must be fit to the  $K_L \rightarrow \pi^0\gamma\gamma$  decay rate. We include the contributions generated by vector meson exchange following the procedure outlined in [5]. In this case the calculation leads to a total branching ratio of

$$B(K_L \rightarrow \pi^0\gamma\mu^+\mu^-) = 5.8 \times 10^{-11}. \quad (4)$$

The decay distributions are presented in Figs. 5 and 6.

For completeness, we also show the double differential branching ratios to  $\mathcal{O}(E^4)$  and  $\mathcal{O}(E^6)$  in Figs. 7 and 8, respectively.

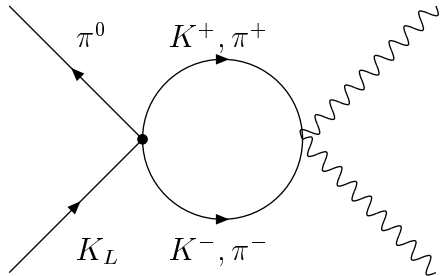
## II. Conclusions

The muonic rate is significantly smaller than the corresponding electronic mode that we studied in Ref. [4]. This is of course due to the more limited phase space, as well as the fact that the photon propagator is further off-shell in the muonic case. However, we again see that the more complete calculation presented second above leads to an enhancement over the purely order  $E^4$  calculation presented first. However, the vector meson diagrams enhance the muonic mode by a significantly smaller factor than either the original di-photon mode or the electronic channel. Thus the prediction in the muonic mode is less useful in deciding on the importance of the vector exchange, although it will be useful in deciding about the overall consistency of the calculation scheme.

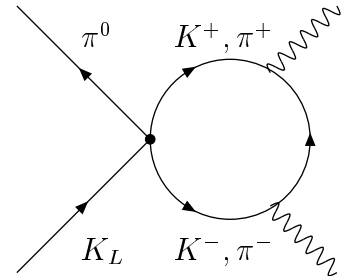
## References

- [1] S. Weinberg, *Physica* **96 A**, 327 (1979); J. Gasser and H. Leutwyler, *Ann. Phys. (N.Y.)* **158**, 142 (1984); *Nucl. Phys.* **B 250**, 465 (1985).
- [2] J. F. Donoghue, B. R. Holstein and G. Valencia, *Phys. Rev. D* **35**, 2769 (1987); G. Ecker, A. Pich and E. de Rafael, *Phys. Lett. B* **189**, 363 (1987); 237 481 1990; *Nucl. Phys. B* **291**, 692 (1987); *Nucl. Phys. B* **303**, 665 (1988); L. Cappiello and G. D'Ambrosio, *Nuovo Cimento* **99 A**, 155 (1988); L. M. Sehgal, *Phys. Rev. D* **38**, 808 (1988); P. Ko and J. Rosner, *Phys. Rev. D* **40**, 3775 (1989); L. Cappiello, G. D'Ambrosio and M. Miragliuolo, *Phys. Lett. B* **298**, 423 (1993); J. Kambor and B. R. Holstein, *Phys. Rev. D* **49**, 2346 (1994); J. F. Donoghue and F. Gabbiani, *Phys. Rev. D* **51**, 2187 (1995); G. D'Ambrosio and J. Portolés, *Nucl. Phys. B* **492**, 417 (1997).
- [3] A. G. Cohen, G. Ecker and A. Pich, *Phys. Lett. B* **304**, 347 (1993).
- [4] J. F. Donoghue and F. Gabbiani, *Phys. Rev. D* **56**, 1605 (1997).
- [5] T. Morozumi and H. Iwasaki, *Prog. Theor. Phys.* **82**, 371 (1989); J. Flynn and L. Randall, *Phys. Lett. B* **216**, 221 (1989); L. M. Sehgal, *Phys. Rev. D* **41**, 161 (1990); P. Ko, *Phys. Rev. D* **41**, 1531 (1990); J. Bijnens, S. Dawson and G. Valencia, *Phys. Rev. D* **44**, 3555 (1991); T. Hambye, *Int. J. Mod. Phys. A* **7**, 135 (1992); P. Heiliger and L. M. Sehgal, *Phys. Rev. D* **47**, 4920 (1993).
- [6] G. Graham and J. Whitmore, private communications.

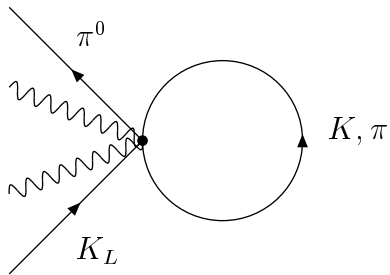
# Figures



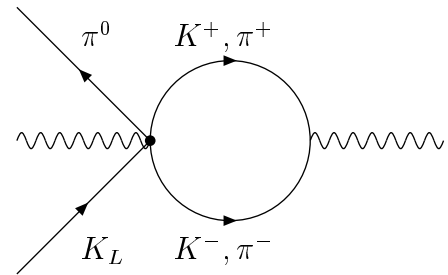
a)



b)



c)



d)

Figure 1: Diagrams relevant to the process  $K_L \rightarrow \pi^0 \gamma \mu^+ \mu^-$  at  $\mathcal{O}(E^4)$  and  $\mathcal{O}(E^6)$ . The muon pair must be attached to one of the photons.

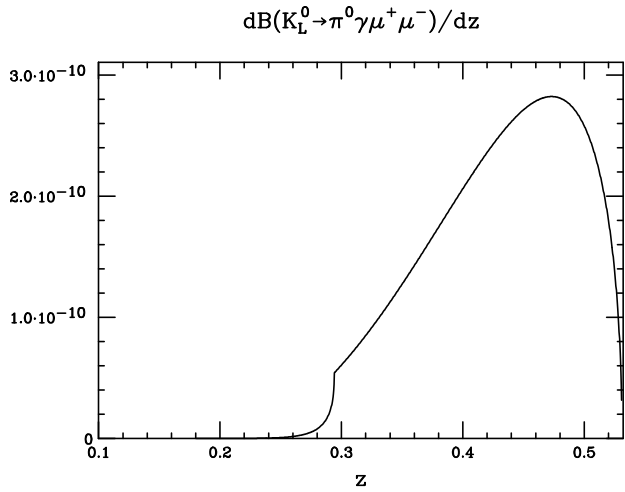


Figure 2: The differential branching ratio  $dB(K_L \rightarrow \pi^0 \gamma \mu^+ \mu^-)/dz$  to order  $E^4$  is plotted vs.  $z$ .

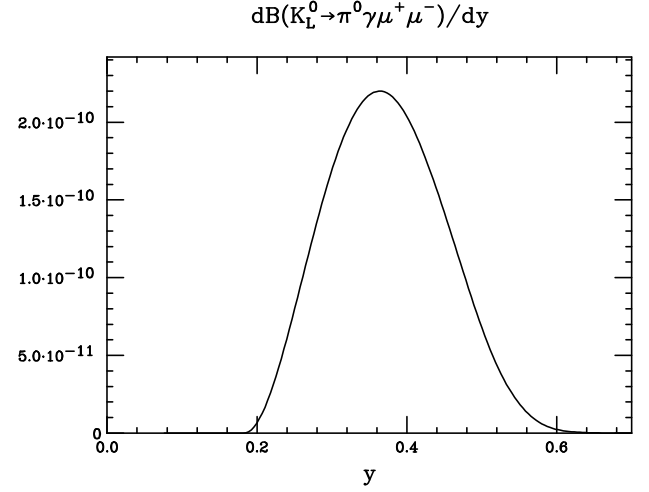
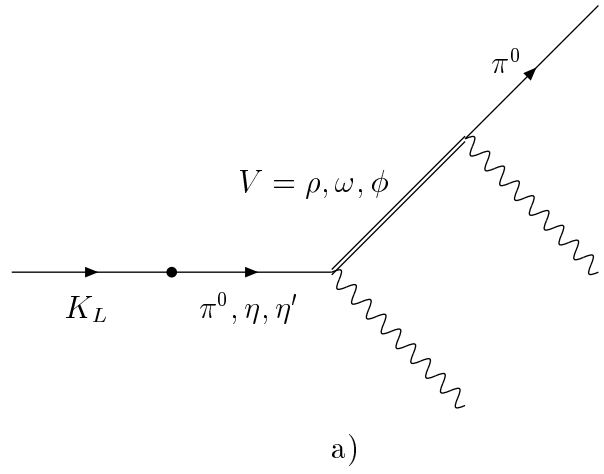
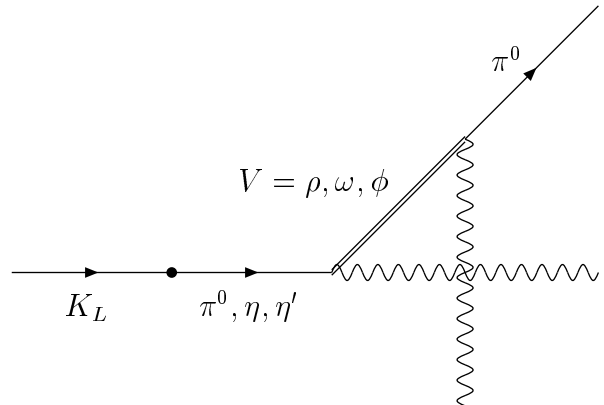


Figure 3: The differential branching ratio  $dB(K_L \rightarrow \pi^0 \gamma \mu^+ \mu^-)/dy$  to order  $E^4$  is plotted vs.  $y$ .



a)



b)

Figure 4: Vector meson exchange diagrams contributing to  $K_L \rightarrow \pi^0 \gamma \mu^+ \mu^-$ .

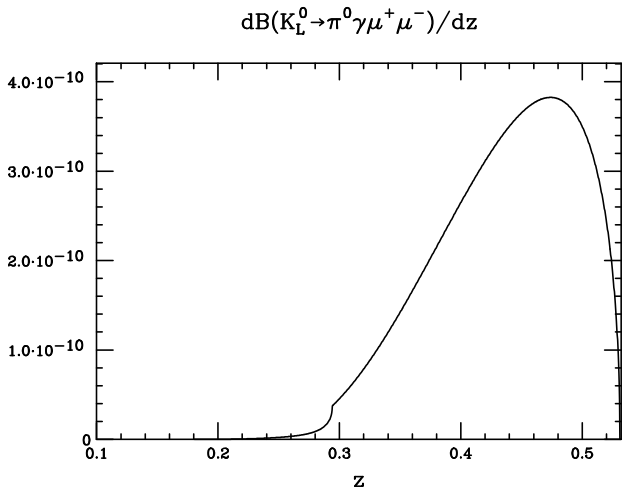


Figure 5: The differential branching ratio  $dB(K_L \rightarrow \pi^0 \gamma \mu^+ \mu^-)/dz$  to order  $E^6$  is plotted vs.  $z$ .

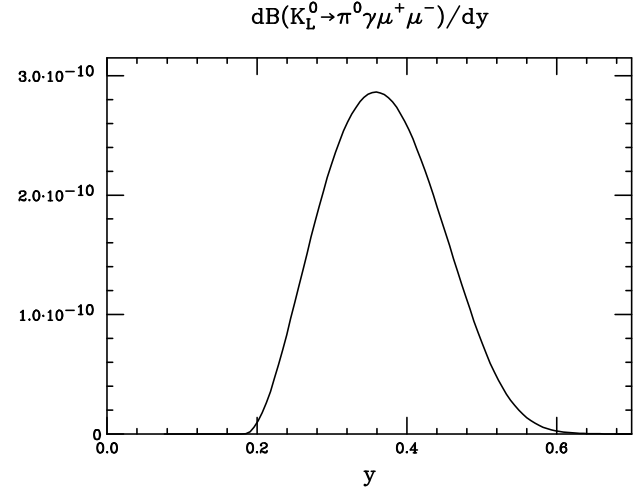


Figure 6: The differential branching ratio  $dB(K_L \rightarrow \pi^0 \gamma \mu^+ \mu^-)/dy$  to order  $E^6$  is plotted vs.  $y$ .

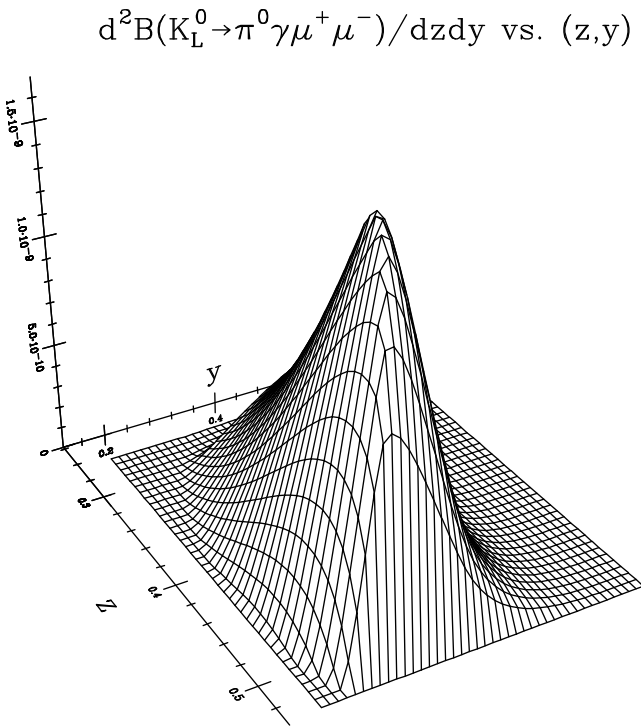


Figure 7: The double differential branching ratio  $d^2B(K_L \rightarrow \pi^0 \gamma \mu^+ \mu^-)/dzdy$  to order  $E^4$  is plotted vs.  $(z,y)$ .

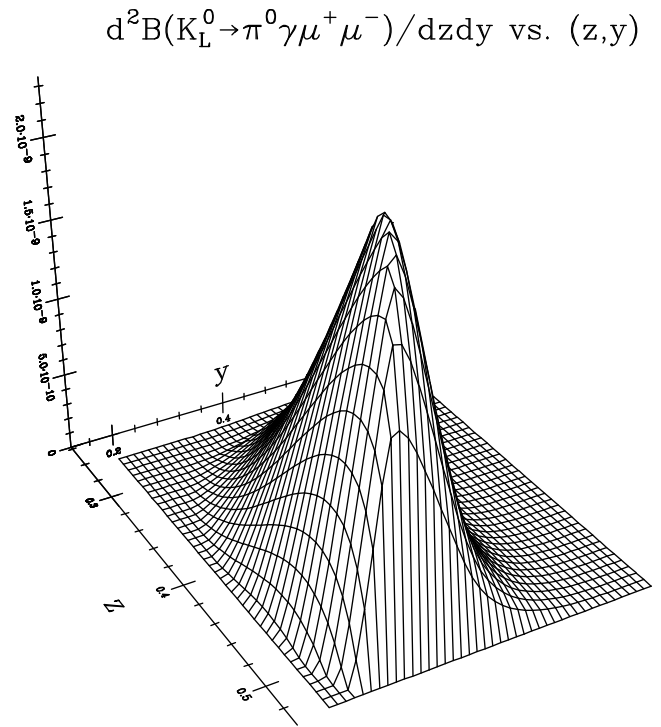


Figure 8: The double differential branching ratio  $d^2B(K_L \rightarrow \pi^0 \gamma \mu^+ \mu^-)/dzdy$  to order  $E^6$  is plotted vs.  $(z,y)$ .